Journal of
Biomolecular Research & Therapeutics

Paban et al., J Biomol Res Ther 2016, 5:3
DOI: 10.4172/2167-7956.1000147

Research Article Open Access

Neuronal and Glial Changes in Rat Hippocampal Formation after Cholinergic Deafferentation

Veronique Paban[1*], Samuel Valable[2], Nathalie Baril[1], Valerie Gilbert[1], Caroline Chambon[1] and Béatrice Alescio-Lautier[1]

[1]*Aix Marseille University, CNRS, LNIA, FR3C, Marseille, France*

[2]*Normandie Univ, UNICAEN, CEA, CNRS, ISTCT/CERVOxy group, Caen, France*

[*]**Corresponding author:** Paban V, Aix Marseille University, CNRS, LNIA, FR3C, Marseille, France, Tel: (33) 413550887; Fax: (33) 4135544; E-mail: veronique.paban@univ-amu.fr

Received date: July 28, 2016; **Accepted date:** September 29, 2016; **Published date:** October 5, 2016

Abstract

The effects of cholinergic insult were studied in the hippocampal formation of cholinergic lesioned rats at metabolic and cellular levels by *in vivo* nuclear magnetic resonance spectrometry and immuno-histochemical approaches. Cholinergic deafferentation was induced by injection of the cholinergic immunotoxin 192 IgG-saporin into the medial septum. The immunotoxin effects were tested at 3, 7, and 30 days post-lesion. Rats with cholinergic deafferentation of the hippocampus showed a lack of NeuN immunoreactivity cells, indicating neuronal loss in hippocampal formation. This neuronal loss was more pronounced in the dentate gyrus, underlining the greater sensitivity of this region to the cholinergic insult. Interestingly, this neuronal loss was not associated with metabolic alteration. These data suggest that the remaining neurons upregulated their functional activity, which would contribute to maintaining the relatively stable level of metabolites and memory abilities. No alteration in GFAP and OX42 immunostaining and in glutamine and myoionositol metabolite concentration was observed in the deafferented regions.

Keywords: 192 IgG-saporin; Hippocampus; Dentate gyrus; NMR spectroscopy; Immunohistochemistry; T maze

Introduction

The cholinergic basal forebrain is an important neuronal system in the brain. It is constituted of two pathways. The first is the septo-hippocampal, which originates in the medial septum and diagonal band of Broca (MS/DBB) and projects to the dentate gyrus and hippocampal fields. Cholinergic neurons of the medial septum innervate the three major cell types of the hippocampus, i.e., pyramidal cells, granule cells, and interneurons, ensuring continual modulatory influence on the hippocampus complex [1]. The second pathway is the basalo-cortical, which originates in the nucleus basalis magnocellularis (NBM) and projects to the entire cortical mantel and the amygdala [2]. Loss of cholinergic input to the hippocampus and cortex is one of the major neuropathological components of the cognitive deficits in Alzheimer's disease [3]. In animals, the study of the cholinergic system was largely improved by the development of the immunotoxin 192 IgG-saporin [4]. The cognitive deficits consecutive to cholinergic lesion depend on many parameters like injection type (intracerebroventricular or intra-structures), lesion extent (MS/DBB lesion, NBM lesion, or global lesion), and task demand [5]. Also, we have previously shown that the behavioural effects of 192 IgG-saporin-induced cholinergic lesion depended on when testing is conducted after surgery [6]. In particular, we demonstrated that at short post-lesion time, less than 1 month, no deficit was observed whereas at longer post-lesion times, from 1 month and up to 1 year, rats showed memory impairments. Although the behavioural effects of cholinergic immune lesion are well established, there are only few data on underlying cellular and molecular events.

The aim of the present study was to critically examine the neuronal and glial changes in the hippocampal formation after cholinergic insult. To do so, *in vivo* magnetic resonance spectroscopy (MRS) and immunohistochemistry were used. To our knowledge, there are no MRS data on the effect of 192 IgG-saporin immune lesion. The immunohistochemistry study was performed to look at many different cellular reactions such as neuronal loss (with neuronal nuclei (Neu-N) staining) and glial reaction (with glial fibrillary acidic protein (GFAP) staining and OX-42 staining). Attention was focused on the hippocampus and the dentate gyrus early in the cholinergic degeneration process, i.e., at 3 or 7 days, which precedes cognitive deterioration, and when cognitive deficit are present, i.e., at 30 days [7].

Experimental Procedures

Animals and surgery

All experiments conformed to international guidelines on the ethical use of animals. Thirty-nine male Long Evans rats (Janvier, France) were used. Nineteen were injected with 192 IgG-saporin (SAP, Chemicon France) and twenty with phosphate buffer saline solution only (PBS). The immunotoxin or PBS was injected bilaterally into the MS/DBB at the following coordinates: From the Bregma, AP+0.4 mm, ML ± 0.0 mm, DV -7.2 mm. The quantity of 192 IgG-saporin was 37.5 ng/side. Rats were 3 months old at the time of the surgery [6-9]. Six groups of rats were then constituted: 2 groups of rats (PBS, N=7 and SAP, N=5) were used at 3 days after surgery, 2 other groups at 7 days (PBS, N=8 and SAP, N=7), and the 2 remaining groups at 30 days (PBS, N=5 and SAP, N=7).

Behavioral analyses

The apparatus was a T-maze made of Plexiglas with a centre stem (72 cm long and 12 cm wide) and 2 side arms (60 cm long and 12 cm wide). The stem was equipped with a guillotine door located 20 cm from the distal end (start box). The entrance to the side arms was equipped with a guillotine door, and at each end there was a food well (1 cm in diameter and 0.75 cm deep). Following a habituation phase, rats learned the nonmatching-to-position protocol. Each trial consisted of paired runs: One forced and one choice run. On the forced run, the side arm was closed by the guillotine door and the other door was open with food pellets placed in the cup. This forced the animal to enter a pre-selected arm and then allowed it to eat the food. Immediately after the forced run, the rat was placed again at the start box for a choice run. At this time, no guillotine door was lowered, and the rat was allowed to choose between the 2 arms. The criterion for scoring an arm visit consisted of the rat placing a hind leg in one of the arms. No backtracking was permitted. When the rat entered the arm opposite to the one rewarded in the forced run (nonmatching), a correct response was recorded, and it was allowed to eat the pellets before returning to its cage. If not, it was confined to the incorrect arm for approximately 20 s, and then returned to its cage. Eight trials were carried out daily until the criterion for acquisition was met. Acquisition was defined as 7 correct trials on 2 consecutive days. A detailed analysis of the learning performance in this behavioural task has already been published [6].

Spectroscopic analyses

Proton MRS was performed on a BRUKER Pharmascan spectrometer 70/16 at 7 Teslas using a dedicated transmits-receive rat head-coil. Rats were anesthetized using a mixture of air (2 L/min) and isoflurane, 3% for induction into a hermetic cage and 2% for maintenance via a nose-cone of a rat head-holder device. Coronal T2-weighted images (turbo-RARE sequence with TE_{eff}=60 ms, TR=2500 ms, rare factor=8, slice thickness=1 mm, FOV=35 mm, matrix=256 × 256, 8 averages) were first acquired for volumetric studies. For volume selective spectroscopy, a PRESS sequence (TE=16 ms; TR=2500 ms; spectral bandwidth=4006.41 Hz, 2048 points, 256 averages) was used to sample a $3 \times 3 \times 3$ mm^3 (27 µL) voxel centered on the coordinate DV of -3.3 mm from bregma. Field homogeneity was adjusted using the FastMap protocol [10], resulting in an 11–15 Hz line width of the water resonance. Data processing was performed using JMRUI (Lyon, France, http://www.mrui.uab.es/mrui). All the spectra were first zero-filled (2048 points) and apodized by a Gaussian function (4 Hz), and metabolite determination was performed using AMARES time-domain fitting procedure. The signal amplitudes corresponding to Nacetylaspartate (NAA), choline/phosphocholine (Cho), glutamate (Glu), myo-inositol (m-Ins), and creatine/phosphocreatine (Cr) were calculated and results were expressed as ratio of the relative area of each metabolite signal to the relative area of Cr. An illustration of spectra from PBS and SAP rats is given in Suppl. Figure A.

Immunohistochemical analyses

At the end of MRS data acquisition, rats were killed and their brains were removed and prepared for immunohistochemistry. Serial sections of 40 µm were prepared for incubation with a goat polyclonal antibody to choline acetyltransferase protein (ChAT) (Chemicon, France, 1:1000), a mouse anti-NeuN (Abcys, France, 1:1000), a goat anti-GFAP (Santa Cruz biotechnology, USA, 1:1000), or a mouse anti-OX-42 (Bachem, UK, 1:1000). After this procedure, sections were incubated in a biotinylated rabbit anti-goat IgG (Vector, France; 1:200) for the ChAT and GFAP stainings and in a biotinylated horse anti-mouse IgG (Vector, France, 1:200) for the NeuN and OX-42 stainings. They were then incubated in an avidin-biotin complex, immersed in a diaminobenzidine H_2O_2 solution, mounted on gelatinized slides, and cover slipped for examination by light microscopy.

Immunoreactivity staining was assessed via computer-assisted image analysis using a Leitz Aristoplan light microscope equipped with a Nikon high-resolution digital camera (756 × 581 pixels) interfaced to a PC computer, Image software (Lucia 5, Nikon) for capturing and processing the images. For each immunoreactivity, the area of the labelled cells was computed by a gray-level method, while adjusting a threshold brightness value. Thus, only immunoreactivity with a gray value above this cutoff was taken into account.

Data analysis for ChAT immunostaining consisted in evaluating the number of labelled cell bodies estimated per surface unit (1 mm^2) in one section at the level of the lesion site, i.e., the MS/DBB, which allowed us to evaluate the effect of the immunotoxin. The surface chosen was always in the same part of the region considered. The boundaries of the brain areas analyzed were defined in accordance with the Paxinos and Watson stereotaxic atlas [11]. ChAT immunostaining was analyzed at a magnification of X5. The lesions produced by 192 IgG-saporin were also determined by staining with cresyl violet to determine the extent of nonspecific damage due to the needle tracks (data not shown).

NeuN immunostaining consisted in evaluating the number of labelled cell bodies. We focused on the pyramidal layer (Pyr) of the CA1 and CA3 regions and on the granular layer (Gra) of the dentate gyrus. The cell number was measured across the total thickness of each layer and in 150 µm of length at magnification X40.

Data analysis for GFAP and OX-42 consisted in evaluating the labelled surfaces. Measures were done in the stratum Oriens (SO) and the stratum Radiatum (SR) layers of the CA1 and CA3 and in the molecular (Mol) and polymorph (PL) layers of the dentate gyrus. The surfaces labelled were measured on a rectangular area of 32925 $µm^2$ at magnification of X40.

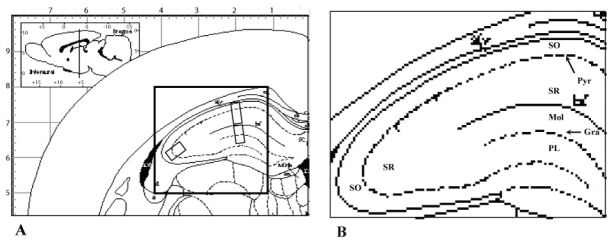

Figure 1: (A) Schematic plate of the rat brain atlas (Paxinos and Watson [11]) at the AP coordinate -3.3 mm from bregma with the voxel position (black square). The three rectangles inside the voxel correspond to the immunolabeled areas measured in the CA1, CA3, and dentate gyrus regions. (B) Schematic representation of the hippocampal complex allowing the distinction of the various strata (SO: Stratum oriens; Pyr: Pyramidal layer; SR: Stratum radiatum; Mol: Molecular layer; Gra: Granular layer; PL: Polymorph layer).

The areas of counting are localized in the voxel position, as shown in Figure 1A. Layers are localized in the hippocampus complex, as shown in Figure 1B.

Statistical analyses

For the behavioral data, a repeated-measures ANOVA was used to analyze the effects of Group and Post-Lesion Time, and their interaction. Further post-hoc comparisons were made using the Newman-Keuls t-test. Differences were considered significant when $P<0.05$.

The results of MRS and immunohistochemistry were analysed with multivariate data analysis using the partial least squares-discriminate analyses (PLS-DA). PLS-DA is a supervised variant of the principal component analysis (PCA). PCA and its related tools have been applied for many decades in epidemiology, econometry, ecology, and cellular biology [12-14]. Although the mathematics behind PCA might seem complex, the basic principle behind it is straightforward, i.e., PCA combines two, or more, correlated factors (i.e., MRS and immunohistochemical data) into one new variable, the principal component (Comp). Thus, in PCA the dimensionality of the dataset is reduced by replacing the original variables by a smaller number of newly formed variables that are a linear combination of the original variables and that explain the majority of the information variability. PLS-DA is a mathematical extension of PCA, where a projection model is developed to predict a Y matrix (in the present case, PLS-DA were run for each post-lesion time, using the 2 groups: PBS and SAP) from the X matrix (MRS and immunohistochemical data). Note that, for that purpose, immunohistochemical data were considered in the whole hippocampal formation. The quality of the model was evaluated using the Q^2 and R^2Y values which are relevant parameters to supervised approaches. Q^2 indicates the predictive capability of the data while R^2Y is a quality factor. Typically, a robust model has a Q^2 value >0.4 and an $R^2Y>0.5$ [15]. The results were visualized by plotting the first two principal components (Comp) of the analysis against each other in a scatter plot, each point representing one animal. With this method, the data also received a variable importance in the projection (VIP) which allows ranking them according to their contribution to the separation. Only data with VIP>1, which are the most influential for the model, are used for further analyses. Unpaired t-test comparison between PBS and SAP groups was used to determine significant changes for each metabolite and immunostaining at each post-lesion time. Differences were considered significant when $P<0.05$.

Results

Behavioral analysis

Behavioral data are shown in Figure 2. An ANOVA computed on the number of days to reach the criterion revealed a Group effect ($F(3,35)=76.72$, $P<0.0001$), a Post-Lesion Time effect ($F(3,35)=80.08$, $P<0.0001$), and a Group x Post-Lesion Time interaction ($F(3,35)=32.97$, $P<0.0001$), showing that depending to the group (PBS or SAP) the number of days to meet the criterion increased as post-lesion time progressed. Newman-Keuls post-hoc comparisons revealed that PBS and SAP rats were significantly different in terms of the number of days to reach the criterion at the post-lesion time of 30 days (Newman-Keuls t-test, $P<0.001$). At the earliest post-lesion time studied, i.e., 3 and 7 days, no difference was observed between PBS and SAP rats.

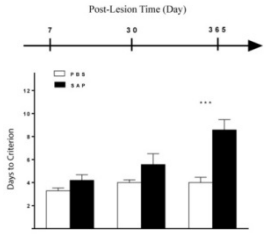

Figure 2: Performance of control (PBS) and 192 IgG-saporin-lesioned (SAP) rats in the nonmatching-to-position as a function of post-operative time. The histograms represent the average (mean ± S.E.M.) numbers of days required to reach the criterion. 192 IgG-saporin-treated rats required significantly more days to reach the criterion than controls at 30 days post-lesion time. ***P<0.001 (vs. PBS group).

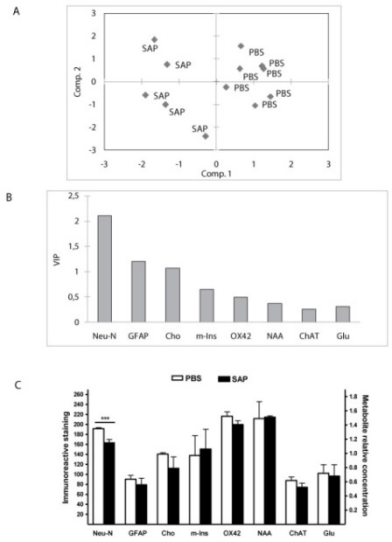

Figure 3: (A) Scatter plot of a PLS-DA analysis of PBS (phosphate buffer saline) and SAP (192 IgG-Saporin) rats at 3 days post-lesion. PLS-DA was run on the MRS and immunostanining data ($Q^2=0.49$ and $R^2Y=0.84$). Each point representing one animal. The first and the second principal components are used, noted Comp1 and Comp2. It showed a clear separation between PBS and SAP rats. From the PLS-DA, data were plotted according to their importance for the separation of groups: with this method, the data received a variable importance in the projection (VIP). Only values greater than 1 are above average and the most relevant. (B) VIP for 3 days post-lesion. (C) Changes of immunostaining (left Y axis) and metabolite relative concentration (right Y axis) in hippocampus in PBS and SAP rats. ***P<0.01, PBS vs. SAP groups (Unpaired t-test). ChAT (choline acetyltransferase), Cho (Choline), GFAP (glial fibrillary acidic protein), Glu (glutamate), m-Ins (myo-inositol), NAA (N-acetylaspartate), NeuN (neuronal nuclei).

MRS and immunohistochemistry analysis At 3 days post-lesion, PLS-DA analyses demonstrated that samples from PBS and SAP rats

were separate (Q^2=0.49, R^2Y=0.84; Figure 3A). The data that predominantly contributed to the separation were Neu-N, GFAP, and Cho (Figure 3B). Group comparison using the unpaired t-test for each data revealed significant differences between PBS and SAP groups only for NeuN immunostaining (t(10)=5.46; p<0.0001). As shown in Figure 3C, NeuN immunostaining was significantly lower in SAP rats relative to PBS rats.

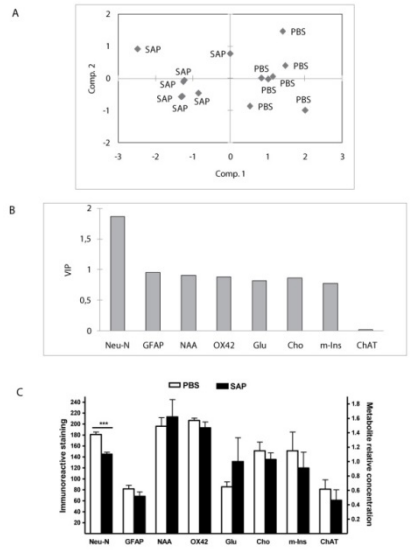

Figure 4: (A) Score plot of a PLS-DA analysis of PBS and SAP rats at 7 days post-lesion. PLSDA was run on the MRS and immunostanining data (Q^2=0.59 and R^2Y=0.73). Samples from SAP rats were separated from those of PBS rats. (B) Corresponding Variable Importance Parameters (VIP). Only values greater than 1 are considered. (C) Changes of immunostaining (left Y axis) and metabolite relative concentration (right Y axis) in hippocampus in PBS and SAP rats. ***P<0.001, PBS vs. SAP groups (Unpaired t-test).

At 7 days post-lesion, the score plot of the PLS-DA model showed separation of PBS and SAP samples (Q^2=0.59, R^2Y=0.73; Figure 4A). The separation was attributed to NeuN staining (Figure 4B). Unpaired t-test for each data revealed significant differences between the two groups of rats for NeuN immunostaining (t(12)=5.68; P<0.0001). Figure 4C shows that NeuN decreased in SAP rats compared to PBS rats.

At 30 days post-lesion, the results obtained using PLS-DA analysis demonstrated that samples from SAP rats were separated from those of PBS rats (Q^2=0.52, R^2Y=0.76; Figure 5A). The data that predominantly contributed to the separation of PBS and SAP rats were ChAT and NeuN (Figure 5B). A comparison between PBS and SAP groups using unpaired t-test revealed significant differences for ChAT (t(10)=3.21; P<0.009) and for NeuN immunostainings (t(10)=3.45; P<0.006). ChAT and NeuN immunostainings were lower in the SAP rats relative to PBS rats (Figure 5C).

Interestingly, the number of NeuN immunoreactive cells was lower in the SAP rats than in the PBS rats at the three post-lesion times in the hippocampal formation. This effect was more pronounced in the dentate gyrus than in the CA1. Indeed, the number of NeuN immunoreactive cells was significantly lower in the SAP rats than in the PBS rats only at 30 days post-lesion in the CA1 (t(10)=3.38, P<0.007; Figure A) and at the three post-lesion times in the dentate gyrus (t(10) ≥ 1.18, P ≤ 0.01; Figure B) (Figure 6). The results of the ChAT immunoreactive cells count are presented in Figure 7. Cholinergic cell loss differed significantly at 30 days post-lesion (t(10)=3.21, P<0.009) between PBS and SAP groups, indicating that the effect of 192 IgG-saporin appeared only at the latest post-lesion time.

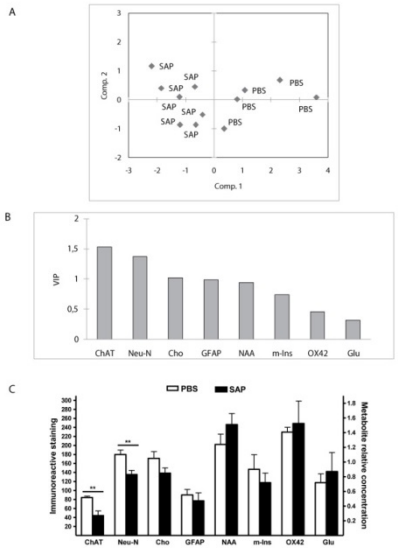

Figure 5: (A) Score plot of a PLS-DA analysis of PBS and SAP rats at 30 days post-lesion. PLSDA was run on the MRS and immunostanining data (Q^2=0.52 and R^2Y=0.76). Samples from SAP rats were separated from those of PBS rats. (B) Corresponding Variable Importance Parameters (VIP). Only values greater than 1 are considered. (C) Changes of immunostaining (left Y axis) and metabolite relative concentration (right Y axis) in hippocampus in PBS and SAP rats. **P<0.01, PBS vs. SAP groups (Unpaired t-test).

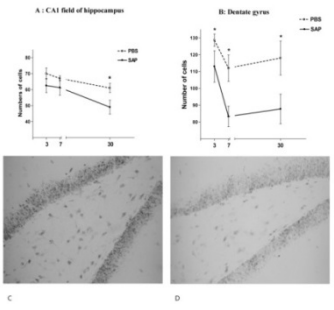

Figure 6: (A) Number of NeuN immunoreactive cells in the pyramidal layer of CA1 and (B) in the granular layer of the dentate gyrus at the three post-lesion times: 3, 7, and 30 days. *P<0.05, PBS vs. SAP groups (Unpaired t-test). Illustration of the NeuN staining in the dentate gyrus in PBS group (C) and in SAP group (D) at 30 days post-lesion.

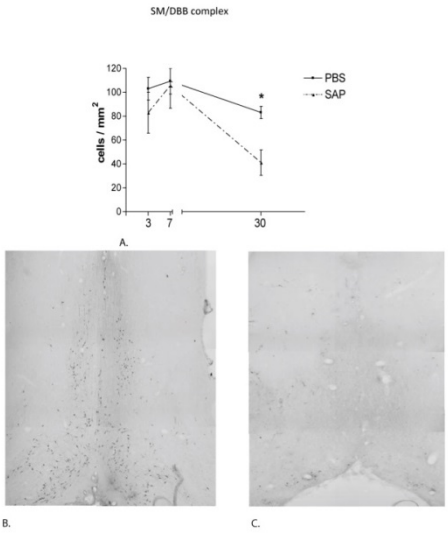

Figure 7: Results of the choline acetyl-transferase (ChAT) immunostaining. Number of ChAT immunoreactive cells in the MS/DBB complex (A) at the three post-lesion times: 3, 7, and 30 days. *Unpaired t-test comparison between PBS and SAP groups. Illustration of the ChAT staining in the MS/DBB complex in PBS group (B) and in SAP group (C) at 30 days post lesion.

Discussion

The cholinergic deafferentation achieved by 192 IgG-saporin injections into the MS/DBB induced a neuronal loss in the hippocampal formation. Immunohistochemical staining of NeuN showed a marked cell loss in the dentate gyrus in particular. NeuN is a neuron-specific nuclear protein expressed in the nucleus and cytoplasm of most neuronal cell types in vertebrate nervous systems. Because of this specific expression, it has come to be regarded as a universal marker for the post-mitotic neuronal phenotype and is used to distinguish neurons from glial and other cells that do not express NeuN [16].

Neuronal loss in the dentate gyrus was observed as soon as 3 days after the 192 IgG-saporin injection, with a maximal loss at 30 days post-lesion. In contrast, in the hippocampus, neuronal loss occurred only at the latest post-lesion times, i.e., when ChAT-immunoreactivity showed a dramatic loss of cholinergic neurons in the MS/DBB. These data suggest that granular cells of the dentate gyrus displayed particular sensitivity to the insult due to cholinergic input. Indeed, these cells were affected even before ChAT neuronal loss was detected. Interestingly, granular cells are activated both by glutamatergic afferents that arrive from the entorhinal cortex via the perforant path and by cholinergic afferents from the medial septum. These cholinergic afferents could be involved in the regulation of granule cell function [17]. Altogether, one may argue that the loss of cholinergic input on granular cells might be responsible for their death. Interestingly, this neuronal loss in the hippocampal formation was not associated with metabolic alteration. This suggests that the remaining neurons had a greater activity, so that the neuronal loss was compensated and stable level of metabolite was maintained. Speculations in this regard are supported by various lesioning models showing that functional activity changes in deafferented postsynaptic structures [18-19].

Immunohistochemical staining of the glial markers, such as GFAP and OX-42, showed no alteration at any post-lesion time. GFAP is the major cytoskeletal protein of glial filaments. It is used as a specific marker for astrocytes [20]. The GFAP positive cells showed typical astroglial morphology of long slender processes and small soma diameter. OX42 recognizes the β2 integrins, CD11b, and CD11c notably, which are well-established markers of microglia [21]. Microglia is composed of long branching processes and a small cellular body. Note that at high magnification, the immunoreactive cells in lesioned rats seemed to be smaller in diameter and shrunk compared to positive cells in non lesioned rats, indicating that cells underwent some alterations.

Metabolites associated with glial cells, such as glutamine and myo-inositol, were not affected. After brain injury, glial hypertrophy or proliferation is usually observed [22-23]. We did not observe such glial reaction in the present study. Note, however, that immunohistochemical and spectroscopic analyses were performed in the projection region, i.e., in the deafferented hippocampus and not in the lesioned site, i.e., the MS/DBB. That may explain this discrepancy. Indeed, glial reaction, when observed, was always reported to be in the lesioned site. Interestingly, astrocytes have been shown to be involved in the modulation of availability, release, and inactivation of glutamate and GABA [24]. Therefore, one may postulate that astrocytes, like neurons, contribute to maintaining a stable level of metabolite.

Results of the present study add to our knowledge concerning brain capacities to respond to cholinergic insult. Indeed, consistent with results from our laboratory in the same hippocampo-dependent paradigm [6], we showed that behavioral deficits appeared only when rats were tested at late post-lesion time, such as 30 days. In contrast, at early post-lesion times (3 and 7 days); the intraparenchymal injection of the immunotoxin did not have behavioral consequences. Correlatively, for animals injected with the 192 IgG-Saporin immunotoxin at the same post-lesion times of 7 and 30 days, we have previously shown neuronal loss of cells expressing c-Fos protein, and more important, an up regulation of the polysialylated neuronal cell adhesion molecule (PSA-NCAM) and brain-derived neurotrophic factor (BDNF) [8-9]. Together, these up regulations of synaptic plasticity and metabolism processes should contribute to sustaining some mnemonic function after cholinergic insult at short post-lesion times. In contrast, when the post-lesion time increases, the remaining neurons cannot face the degenerative processes anymore. The residual system is not able anymore to compensate the neuronal loss, resulting in behavioral deficit.

References

1. Ge S, Dani JA (2005) Nicotinic acetylcholine receptors at glutamate synapses facilitate long term depression or potentiation. J Neurosci 25: 6084-6091.
2. Mesulam MM, Mufson EJ, Wainer BH, Levey AI (1983) Central cholinergic pathways in the rat: an overview based on an alternative nomenclature (Ch1-Ch6). Neuroscience 10: 1185-1201.
3. Gaykema RP, Nyakas C, Horvath E, Hersh LB, Majtenyi C, et al. (1992) Cholinergic fiber aberrations in nucleus basalis lesioned rat and Alzheimer's disease. Neurobiol Aging 13: 441-448.
4. McGaughy J, Everitt BJ, Robbins TW, Sarter M (2000) The role of cortical cholinergic afferent projections in cognition: impact of new selective immunotoxins. Behav Brain Res 115: 251-263.

5. Parent MB, Baxter MG (2004) Septohippocampal acetylcholine: involved in but not necessary for learning and memory? Learn Mem 11: 9-20.
6. Paban V, Chambon C, Jaffard M, Alescio-Lautier B (2005) Behavioral effects of basal forebrain cholinergic lesions in young adult and aging rats. Behav Neurosci 119: 933-945.
7. Paban V, Jaffard M, Chambon C, Malafosse M, Alescio-Lautier B (2005) Time course of behavioral changes following basal forebrain cholinergic damage in rats: Environmental enrichment as a therapeutic intervention. Neuroscience 132: 13-32.
8. Paban V, Chambon C, Manrique C, Touzet C, Alescio-Lautier B (2011) Neurotrophic signaling molecules associated with cholinergic damage in young and aged rats: environmental enrichment as potential therapeutic agent. Neurobiol Aging 32: 470-485.
9. Chambon C, Paban V, Manrique C, Alescio-Lautier B (2007) Behavioral and immunohistological effects of cholinergic damage in immunolesioned rats: Alteration of c-Fos and polysialylated neural cell adhesion molecule expression. Neuroscience 147: 893-905.
10. Gruetter R (1993) Automatic, localized *in vivo* adjustment of all first- and second-order shim coils. Magn Reson Med 29: 804-811.
11. Paxinos G, Watson C (1998) The Rat Brain in Stereotaxic Coordinates. Academic Press.
12. Belzung C, Le Pape G (1994) Comparison of different behavioral test situations used in psychopharmacology for measurement of anxiety. Physiol Behav 56: 623-628.
13. Cadet F (1999) Measurement of sugar content by multidimensional analysis and mid-infrared spectroscopy. Talanta 48: 867-875.
14. Franke K, Ziegler G, Klöppel S, Gaser C (2010) Estimating the age of healthy subjects from T(1)-weighted MRI scans using kernel methods: Exploring the influence of various parameters. Neuroimage 50: 883-592.
15. Eriksson T (1999) Executive Compensation and Tournament Theory: Empirical Tests on Danish Data. J Labor Eco 17: 262-280.
16. Wolf HK, Buslei R, Schmidt-Kastner R, Schmidt-Kastner PK, Pietsch T, et al. (1996) NeuN: a useful neuronal marker for diagnostic histopathology. J Histochem Cytochem 44: 1167-1171.
17. Leranth C, Hajszan T (2007) Extrinsic afferent systems to the dentate gyrus. Prog Brain Res 163: 63-84.
18. Kharatishvili I, Immonen R, Gröhn O, Pitkänen A (2007) Quantitative diffusion MRI of hippocampus as a surrogate marker for post-traumatic epileptogenesis. Brain 130: 3155-3168.
19. Ziaja M, Pyka J, Machowska A, Maslanka A, Plonka PM (2007) Nitric oxide spintrapping and NADPH-diaphorase activity in mature rat brain after injury. J Neurotrauma 24: 1845-1854.
20. Pekny M, Pekna M (2004) Astrocyte intermediate filaments in CNS pathologies and regeneration. J Pathol 204: 428-437.
21. Guillemin GJ, Brew BJ (2004) Microglia, macrophages, perivascular macrophages, and pericytes: a review of function and identification. J Leukoc Biol 75: 388-397.
22. Steen RG, Ogg RJ (2005) Abnormally high levels of brain N-acetylaspartate in children with sickle cell disease AJNR. Am J Neuroradiol 26: 463-468.
23. Shutter L, Tong KA, Holshouser BA (2004) Proton MRS in acute traumatic brain injury: role for glutamate/glutamine and choline for outcome prediction. J Neurotrauma 21: 1693-1705.
24. Schousboe A, Waagepetersen HS (2006) Glial modulation of GABAergic and glutamatergic neurotransmission. Curr Top Med Chem 6: 929-934.